22nd IMEKO TC4 International Symposium & 20th International Workshop on ADC Modelling and Testing
SUPPORTING WORLD DEVELOPMENT THROUGH ELECTRICAL&ELECTRONIC MEASUREMENTS
IASI, ROMANIA, September 14-15, 2017

Magnetic Field Effects on Human Bodyof Wireless Chargers for E-bikes

M. Caruso, V. Castiglia, R. Miceli, F. Pellitteri,C. Spataro and F. Viola

Department of Energy, Information Engineering and Mathematical Models, University of Palermo, Viale delle Scienze, Building n. 9, 90128 Palermo (Italy)

Abstract – For the electric vehicles battery charging, the wireless power transmission is increasingly representing an innovative solution. The inductive power transfer is the standard technology of wireless charging: the energy transfer occurs between two magnetically coupled coils. Although this battery charging system is especially convenient for E-bikes, the physiological effects of the related magnetic fields shall be estimated and taken into account. In this paper, a 200 W prototype of wireless battery charger for E-bikes is proposed and described. Moreover, various measurements of the surrounding magnetic field are carried out to evaluate the actual physiological compatibility of the system.

Keywords –electric bicycles, inductive power transfer, wireless battery charging, magnetic fields

I. INTRODUCTION

Nowadays, thanks to the unremitting diffusion of Electric Vehicles (EVs),highly innovative, fast and cheap methods for battery charging, are increasingly proposed and tested.

One of these is based on the wireless energy transmission, through Inductive Power Transfer (IPT): the electrical power arising from the mains is addressed to the vehicle battery via magnetic coupling between a primary and a secondary winding [1-2].

The wireless solution provides significant benefits in terms of comfortable operation and electrical safety. The absence of power cords makes the charging activation easier, preventing the driver from managing any bothersome plug-in operation. Moreover, the user is saved from handling power cables, a potentially dangerous operation.

The wireless battery charging is able to provide also logistic benefits, since the vehicle could be supplied during its motion and postpone its need to be recharged. Therefore, dynamic EVs charging may bring enormous advantages in terms of vehicle autonomy and battery mass lightening [3-4].

The IPT-based battery charging is implemented through the magnetic coupling between two winding coils lying on two parallel pads, which are in general placed in the following way: the power transmitter pad is placed under the bottom of the vehicle; the power receiver pad is placed on the road [5-8].

The IPT represents a viable solution for the Vehicle-To-Grid (V2G) concept [9-11]. According to V2G, the vehicle is used as a storage element for other electrical loads of the mains: a bi-directional power transfer is feasible, since the power can flow from the electrical mains to the vehicle battery or in the opposite direction, based on the battery status and the grid energy requests [12-13].

Without any doubt, the wireless charging solution is particularly cost-effective and convenient for the E-bike application. In fact, the infrastructural cost required in order to build,manageand maintain IPT stalls for electric bicycles would be modest if compared to the case of cars and buses. Moreover, E-bikes require low power levels, compared to the electric cars: while an E-car requires at least 3 kW, an electric bicycle requires at least 100 W to be charged. In comparison with other EVs, however, only few works have been presented in scientific literature concerning the IPT for E-bike battery charging [13-14].

In spite of the different advantages provided by the wireless solution for battery charging, some care shall be addressed towards the exposure to the magnetic field related to the inductive coupling, which has not been extensively studied yet.

In this context, this paper presents a contactless power transfer prototype for E-bike charging, from its design to the experimental investigation on its physiological compatibility.

More in detail, some comments are initially provided in Section II in order to describe the proposed system. Afterwards, the issue of the magnetic field exposure is investigated, with the aim of characterize the region surrounding the IPT device, at a fixed distance from the center of the system and on the distances of compliance with the ICNIRP standards [15]. Experimental results are given in Section III, obtained through several sets of measurement in order to investigate the sensibility of the system to the most significant parameters involved during its operation.

II. PROBLEM STATEMENT

The effects on the human body of the magnetic field produced by the IPT system shall be investigated. An accurate evaluation of the potential risks arising from the exposure to magnetic flux density in an EV wireless charger depends on the specific vehicle taken into consideration.

For this purpose, the ICNIRP guidelines have been taken into account [15]. These guidelines have been established to provide protection against adverse health effects arising from electric and magnetic fields exposure. Both direct and indirect effects have been considered by ICNIRP: direct effects arise from the interaction between the fields and the body, whereas indirect effects concern the interaction with a conducting object having an electric potential different from that of the body. These guidelines do not involve product performance standards and, therefore, do not specifically intend to limit emissions from devices.

Therefore, a set of measurements on a specific wireless charging system for E-bikes has been carried out in order to investigate the magnetic field distribution. The main goal is the definition of a safety distance from the IPT system.

Fig. 1 shows the model of the DC-DC stage of the proposed IPT system. The electrical power can flow from the DC-link to the rechargeable battery or in the reverse direction, since the system is bi-directional.No ferromagnetic core has been used for each of the flat and round coils, so that the structure is light-weight. In Table 1, each coil is geometrically characterized: d and l are the section diameter and the total length of the wire, whereas N and d_{out} are respectively the number ofturns and the outer diameter of the coil. The technical features of the IPT system are summarized in Table 2.

The magnetically coupled coils in which the power transfer is provided are characterized by the primary and secondary self-inductances, namely L_1 and L_2, respectively, and the mutual inductance M. The coils are loosely coupled due to the presence of the air-gap.

Table 1. Geometrical Data of the coils

Parameter	Value
d	3 mm
l	3.48 m
N	9
d_{out}	15 cm

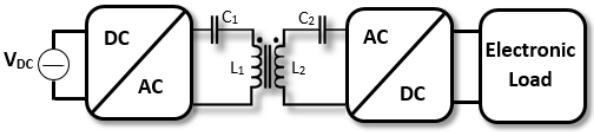

Fig. 1. Model of the DC-DC stage of the IPT system

Table 2. Electrical features of the IPT system

Element	Value
$L_1=L_2=L$	15.6 µH
M_{airgap}	9.6µH (1 cm)
	6.6µH (2 cm)
	4.9µH (3 cm)
$C_1 = C_2 = C$	250 nF
V_{Load}	20 V

Therefore, a reactive compensation network composed by the capacitors C_1 and C_2 is required so that the power transfer efficiency is maximized and the power factor is optimized.

To achieve the double goal of maximum power factor and maximum power transfer, the resonant frequency of the primary LC filter is chosen equal to the resonant frequency of the secondary LC filter. Therefore, being L_1 and L_2 equal to each other, the series capacitances C_1 and C_2 are chosen equal to each other as well.

Being C the common value of capacitance, the frequency f is given by:

$$f = \frac{1}{2\pi\sqrt{LC}} \qquad (1)$$

A 200 W load power has been chosen with a resonant frequency equal to 85 kHz.

According to ICNIRP guidelines, as shown by Table 3, the RMS value of magnetic flux density B_{rms}, which should be considered as the maximum limit for general public exposure, is 27 µT at the frequency of 85 kHz.

Table 3. ICNIRP guidelines concerning the general public exposure: the RMS limit for the magnetic flux density is highlighted.

Frequency range	E-field strength E (kV m^{-1})	Magnetic field strength H (A m^{-1})	Magnetic flux density B (T)
1 Hz–8 Hz	5	$3.2 \times 10^4/f^2$	$4 \times 10^{-2}/f^2$
8 Hz–25 Hz	5	$4 \times 10^3/f$	$5 \times 10^{-3}/f$
25 Hz–50 Hz	5	1.6×10^2	2×10^{-4}
50 Hz–400 Hz	$2.5 \times 10^2/f$	1.6×10^2	2×10^{-4}
400 Hz–3 kHz	$2.5 \times 10^2/f$	$6.4 \times 10^4/f$	$8 \times 10^{-2}/f$
3 kHz–10 MHz	8.3×10^{-2}	21	2.7×10^{-5}

III. EXPERIMENTAL TESTS AND RESULTS

In order to experimentally validate the statements described in the previous Sections, a test bench was assembled and Fig. 2 shows its photograph. It is mainly composed by:

- a transmitter board with a MOSFETS full-bridge inverter connected to the primary coil;
- a receiver board with a MOSFETS full-bridge active rectifier connected to the secondary coil;
- a DC voltage source (Hewlett Packard Enterprise), which is used to supply the full-bridge and the MOSFET drivers of the transmitter board;
- a Spartan-3A FPGA board, which is used to generate the inverter and rectifier commands;
- an AGILENT 6060B 300 W variable electronic load;
- aYOKOGAWA DL1740*oscilloscope*, which is used for the real-time waveform detection and measurement of the main electrical quantities involved in the proposed system;
- a wide frequency range (1 Hz - 400 kHz) NARDAELT 400 exposure level tester, equipped with a 3 cm^2 ELT B-field probe.

The schematic representation of the bench is shown in Fig.3, whereas a photograph of the coils built for the IPT system is given in Fig. 4.

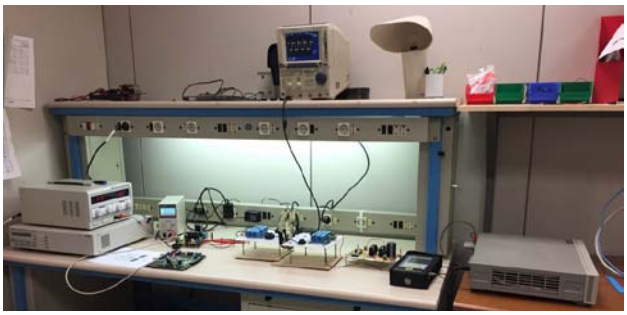

Fig. 2. The test bench

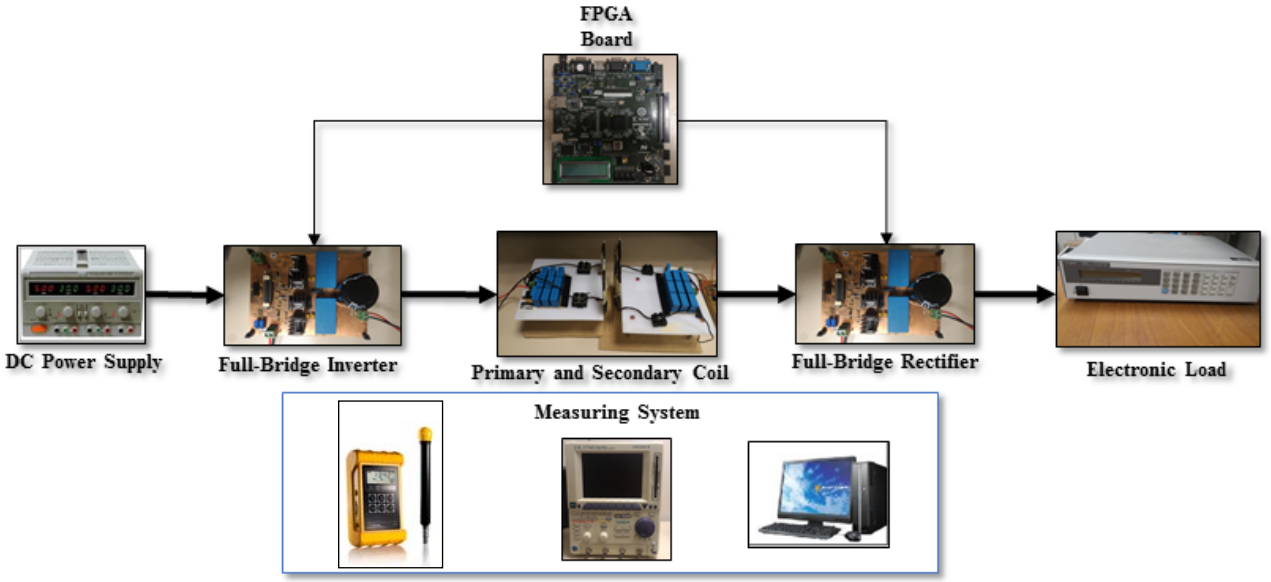

Fig. 3. Schematic representation of the proposed test bench

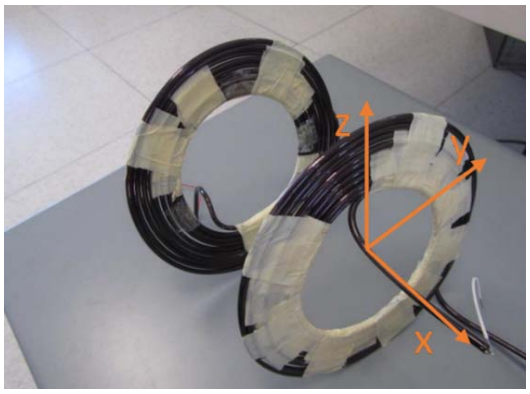

Fig.4. Photograph of the coils built for the IPT system

An experimental investigation on the magnetic flux density values in the regions surrounding the devicewas provided by measuring the magnetic flux density in three different points. According to the procedure described in [16], the estimated expanded (k=2) uncertainty for the magnetic flux density measurements is 8%.By choosing the reference axis as shown in Fig. 4, the three points, indicated with Pi (x,y,z) [cm] are:

- Point P1 (15,0,0);
- Point P2 (0,15,0);
- Point P3 (0,0,15).

The first set of measurement (set nr.1) consists in operating the device at its maximum power of 200 W and changing the air gap between the two inductors. More in detail, three different distances have been chosen: 1 cm, 2 cm and 3 cm. For each position,the corresponding flux density field values are reported in Table 4. These results can be also graphically appreciated from Fig. 5. In table 4 are reported also the overall efficiency η_{tot} of the power transfer system that is the product of the DC/AC efficiency, the coupling efficiency and the AC/DC efficiency.

Table 4. Measured B at different points with output power of 200 W

Air Gap [cm]	**η_{tot} [%]**	**Magnetic flux density [μT]**			**Safety Distance[cm]**
		P1	**P2**	**P3**	
1	77	28	20	19	16
2	68	29	23	21	17
3	57	30	27	20	18

As shown from Table 4, most of the points featuring values higher than the ICNIRP limit of 27 μT belong to the point P1, corresponding to the x-axis. Since the x-axis represents the worst case regarding the magnetic flux density, the distance has been increased until the field is reduced to 27 μT (Safety Distance). For each value of the air gap, the corresponding Safety Distance is reported in the last column of Table 4.

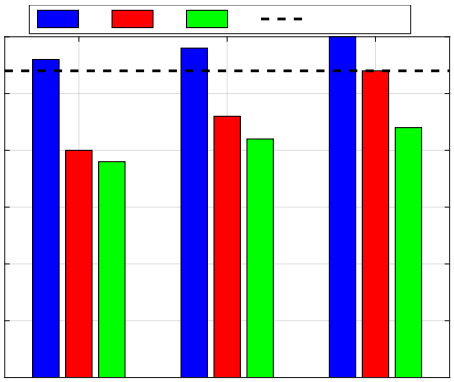

Fig.5. Experimental results for set nr.1

Another set of experimental results (set nr.2) has been performed by varying the output power of the prototype from 50 W to 150 W with steps of 50 W. For each power value, the same investigation on the flux density surrounding the prototype above described (set nr.1) and Table 5 summarizes the measured values of |B|, whereas Fig. 6the magnetic flux density measured in P1 with different air gaps and output power.

As expected, it can be noticed that, by increasing the output power, the ICNIRP limit is reached at a higher distance. Therefore, the safety distance limit is also related to the electrical power of the wireless power transfer system.

As the magnetic field values were greater with an air gap of 3 cm, at the maximum output power of 200 W, subsequent measurements were made by fixing these conditions.

Other interesting results have been obtained with a third set of measurements (set nr.3), in which a displacement of the magnetic axes of the coils has been provided. This misalignment was varied between ±0.5 cm to ±2 cm with steps of 0.5 cm along the y axis of the coils.

Table 6 summarize the measured values of |B|, whereas Fig. 7 provides a graphical view of these results.The system has almost a symmetrical behavior with respect of point P1 (x axis) and point P3 (z axis).

Finally, in order to verify the sensibility of the system towards frequency variations with respect to its resonant frequency, another set of measurements has been carriedout (set nr.4), consisting of measuring the flux density at the safety distance point (18 cm from Table 4) by changing the operation frequency in the range ± 5 kHz of the resonant frequency with steps of 1 kHz. Table 7 summarizes the obtained results, which can be graphically appreciated from Fig. 8. The magnetic field varies with frequency; in particular, it decreases as the frequency increases. Therefore, to maintain the magnetic field below the ICNIRP limits, it is important not to change the frequency.

Table 5. Measured B for set nr.2

Output Power [W]	η_{tot} [%]	Air Gap [cm]	Magnetic flux density [μT]			Safety Distance [cm]
			P1	P2	P3	
50	74	1	16	12	10	11
	65	2	18	16	13	12
	56	3	20	18	14	13
100	74	1	21	15	12	12
	66	2	23	20	13	13
	56	3	25	22	15	14
150	75	1	24	17	13	14
	67	2	26	20	15	15
	56	3	28	25	18	16

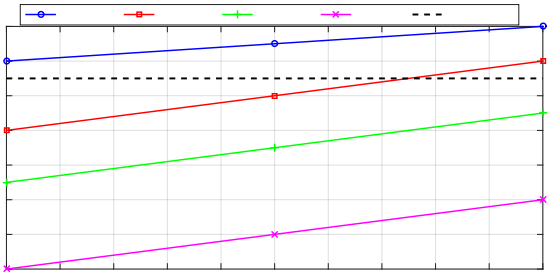

Fig.6. Experimental results for set nr.2

Table 6. Measured B for set nr.3

Misalignment [cm]	η_{tot} [%]	Magnetic flux density [μT]		
		P1	P2	P3
-2	53	32	21	28
-1.5	55	31	22	25
-1	57	30	24	24
-0.5	57	29	25	22
0.5	57	29	26	22
1	56	30	28	26
1.5	55	31	30	28
2	53	33	32	30

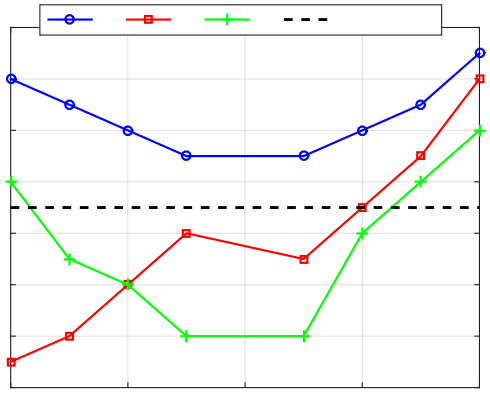

Fig.7. Experimental results for set nr.3

Table 7. Measured B for set nr.4

Frequency [kHz]	η_{tot} [%]	Magnetic flux density [μT]
80	46	35
81	51	33
82	54	31
83	57	30
84	57	29
85	57	27
86	57	26
87	56	25
88	54	24
89	50	23
90	45	22

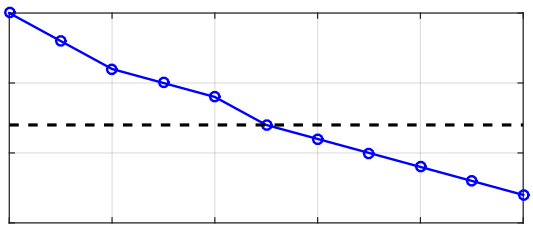

Fig.8. Experimental results for set nr.4

IV. CONCLUSIONS

This paper has presented the results of a detailed experimental study on the physiological compatibility of the proposed wireless charger for electric bikes.

The physiological effects of the related magnetic fields generated by the prototype have been measured and from the experimental results it can be stated that the proposed system needs better coil design and needs shielding to keep the magnetic flux density below the ICNIRP limit in all the operating conditions. By modifying the output power, the misalignment or the operating frequency, the magnetic flux density limits are not always respected. For this reason, a safety distance corresponding to 25 cm is suggested from the center of the device during charging operations.

V. ACKNOWLEDGMENTS

This work was financially supported by MIUR - Ministero dell'Istruzione, dell'Università e della Ricerca (Italian Ministry of Education, University and Research) and by SDESLab (Sustainable Development and Energy Saving Laboratory) of the University of Palermo.

REFERENCES

[1] M. Budhia, G. A. Covic, and J. T. Boys, *Design and optimization of circular magnetic structures for lumped inductive power transfer systems*,IEEE Trans. Power Electron., vol. 26, no. 11, pp. 3096–3108, Nov. 2011.

[2] J. Sallan, J. L. Villa, A. Llombart, and J. F. Sanz, *Optimal Design of ICPT Systems Applied to Electric Vehicle Battery Charge*, Industrial Electronics, IEEE Transactions on, vol. 56, pp. 2140–2149, 2009.

[3] T. Diekhans, R. W. De Doncker, *A Dual-Side Controlled Inductive Power Transfer System Optimized for Large Coupling Factor Variations and Partial Load*,IEEE Trans. Power Electron., vol. 30, no. 11, pp. 6320-6328, Jan. 2015.

[4] S. Choi, J. Huh, W. Y. Lee, S. W. Lee, and C. T. Rim, *New cross-segmented power supply rails for roadway-powered electric vehicles*,IEEE Trans. Power Electron., vol. 28, no. 12, pp. 5832–5841, Dec. 2013.

[5] J. G. Taiber, *Advances in wireless charging of electrified vehicles and need for standardization*,Proc. of IEEE PES Innovative Smart Grid Technologies Conference (ISGT), Feb. 2014.

[6] S. Chopra, and P. Bauer, *On-road contactless power transfer - case study for driving range extension of EV*, in Proc. of Industrial Electronics, 2011. IECON '11. 37th Annual Conference of IEEE, 2011, pp. 4596–4602.

[7] J. Huh, S. Lee, C. Park, G.-H. Cho, and C.-T. Rim, *High performance inductive power transfer system with narrow rail width for On-Line Electric Vehicles*,in Proc. of Energy Conversion Congress and Exposition (ECCE), 2010 IEEE, 2010, pp. 647–651.

[8] T. Yiyun, L. Can, C. Lin, and L. Lin, *Research on Vehicle-to-Grid Technology*,in Proc. ofComputer Distributed Control and Intelligent Environmental Monitoring (CDCIEM), 2011 International Conference on, Feb. 2011, pp. 1013-1016.

[9] U. K. Madawala and D. J. Thrimawithana, *A Bidirectional Inductive Power Interface for Electric Vehicles in V2G Systems*,Industrial Electronics, IEEE Transactions on, vol. 58, pp. 4789–4796, 2011.

[10] U. K. Madawala, M. Neath, and D. J. Thrimawithana, *A Power-Frequency Controller for Bidirectional Inductive Power Transfer Systems*, Industrial Electronics, IEEE Transactions on, vol. 60, pp. 310-317, 2013.

[11] U. K. Madawala, and D. J. Thrimawithana,*Current sourced bi-directional inductive power transfer system*, Power Electronics, IET, vol. 4, pp. 471-480, 2011.

[12] H. Z. Beh, G. A. Covic, and J. T. Boys, *Magnetic couplers in kickstands for wireless charging of electric bicycles*,in Proc. of Applied Power Electronics Conference and Exposition (APEC), 2014 Twenty-Ninth Annual IEEE, 2014, pp. 1348-1355.

[13] F. Pellitteri, V. Boscaino, R. Miceli, and U. K. Madawala, "Power tracking with maximum efficiency for wireless charging of E-bikes," in Electric Vehicle Conference (IEVC), 2014 IEEE International, 2014, pp. 1–7.

[14] H. Jiang, P. Brazis, M. Tabbador, and J. Bablo, *Safety considerations of wireless charger for electric vehicles — A review pape*r, in Proc. ofProduct Compliance Engineering (ISPCE), 2012 IEEE Symposium on, 2012, pp. 1-6.

[15] International Commission on Non-Ionizing Radiation Protection, *Guidelines for limiting exposure to time-varying electric and magnetic fields (1 Hz–100 kHz)*,Health Phys., vol. 99, no. 6, pp. 818–836, 2010.

[16] S. Caldara, R. Miceli, P. Romano, C. Spataro and F. Viola, *Uncertainty management in the measurements of low frequency magnetic fields*, in Proc. of20th IMEKO TC4 International Symposium Benevento, Italy, September 15-17, 2014.